Research Square

Preprints are preliminary reports that have not undergone peer review.
They should not be considered conclusive, used to inform clinical practice,
or referenced by the media as validated information.

Threshold proline decline predicts coordinated stomatal–non- stomatal recovery in soybean after drought rewatering

Sergio Da Silva
Stellenbosch University
Ashwil Klein
University of the Western Cape
Itumeleng Moroenyane
imoroenyane@sun.ac.za

Stellenbosch University

Short Report

Keywords: drought recovery, proline, Bayesian hierarchical model, stomatal limitation, one-point Vcmax, LI-6800, threshold dose–response, Glycine max

Posted Date: October 21st, 2026

DOI: https://doi.org/10.21203/rs.3.rs-11121207/v1

License: This work is licensed under a Creative Commons Attribution 4.0 International License.
Read Full License

Additional Declarations: No competing interests reported.

Abstract

Objective. Rehydration after drought reveals two coupled processes: catabolic clearance of osmolytes accumulated during stress, and the resumption of photosynthesis by stomatal re-opening and biochemical recovery [1]. We asked whether these processes respond to prior stress severity continuously or beyond a threshold, using a five-level pilot in *Glycine max* re-watered to 100% of field capacity and sampled on day 2 of recovery.

Results. A hierarchical Bayesian model with joint calibration estimated leaf proline in the extreme-stress plant to be 75 µg g^{-1} FW lower than the never-stressed control (95% credible interval −132 to −12; posterior probability of a decrease = 0.985), whereas mild-, moderate-, and severe-stress plants did not differ from the control. A hinge model located a change-point between the severe and extreme levels (θ = 3.9, 95% CrI 2.4–4.7) and out-predicted a linear decline (ΔELPD = 2.2 ± 1.2). Diurnal gas exchange after correcting a widespread leaf-area error (which had inflated C□ by 199 µmol mol^{-1} and placed 21 of 24 values above ambient CO_2) showed non-stomatal effects accounted for 78–94% of leaf-to-leaf differences in assimilation, while apparent V_{cmax} tracked stomatal conductance across the day (ρ = 0.90). Findings apply to these five plants; replication with continuous severity is required.

Introduction

Plants surviving drought must both restore carbon assimilation and clear the osmolytes and signals accumulated during stress. Proline accumulates during dehydration through P5CS induction and is oxidised on rehydration by proline dehydrogenase, so residual leaf proline after re-watering reports the balance between prior stress and catabolic recovery [2, 3]. Photosynthesis recovers on two partly separable axes: stomatal re-opening, which abscisic acid can hold back after hydraulic status is restored [4, 5], and restoration of mesophyll and biochemical capacity, which lags after severe stress [1, 6, 7]. Whether these processes respond to stress severity continuously or beyond a threshold determines how recovery should be modelled and which regulators to target, including the root-derived CLE25 peptide that acts upstream of foliar ABA biosynthesis [8].

We report a pilot experiment in soybean (*Glycine max*) that combines diurnal LI-6800 gas exchange with a proline assay on the same leaf, two days after re-watering plants from five levels of prior soil drying (T1 control to T5 extreme). The design is deliberately small: one plant per severity level, top (third) trifoliate, day 2 after re-watering to 100% field capacity. We test four hypotheses: H1, residual proline declines only beyond a severity threshold; H2, early photosynthetic recovery is limited by diffusion (stomatal re-opening); H3, the diurnal maximum of stomatal conductance shifts later after more severe stress; H4, proline status predicts diurnal carbon gain. We formulate H1 as a Bayesian model comparison that propagates calibration uncertainty into every treatment estimate, and H2 as an exact log-ratio partition of leaf-to-leaf differences in assimilation into diffusive and non-stomatal components. The exercise also evaluates a post-hoc correction to LI-6800 outputs for partially filled chambers.

Methods

Plants and treatments.

Soybean plants at the same developmental stage (R1) were exposed to five levels of soil drying (T1 well-watered control to T5 extreme drought) followed by re-watering to 100% pot capacity (wet sand) and sampled on day 2 of recovery from the top (third) trifoliate. Two proline extracts per plant, each read in triplicate wells, were prepared; T5 plants survived but were not considered for gas exchange analysis. Figure 1a shows the experimental design used in this pilot study.

Gas exchange.

A LI-6800 (LI-COR, 6800-12 chamber) recorded six rounds on the T1–T4 trifoliate leaves between 07:19 and 17:09 using the following parameters: PAR 1000 µmol m^{-2} s^{-1}, reference CO_2 415 µmol mol^{-1}, flow 300 µmol s^{-1}. Leaves filled 4.8–6.1 cm^2 of the 9 cm^2 aperture. Because assimilation, transpiration and total conductance scale with 1/S, we multiplied each by 9/S and recomputed g_{tv} and C_i from the instrument's equations [9] rather than rescaling C_i itself (implementation reproduced logged C_i within 1 µmol mol^{-1} at S = 9). We estimated apparent V_{cmax} per log with the one-point method [10] using standard temperature functions [11] and computed stomatal limitation $L_s = 1 - A/A(C_i = C_a)$ [12, 13]. For every leaf and round we partitioned ln(A_leaf/A_T1) exactly into a diffusive term, ln[f(C_i)_leaf/f(C_i)_T1], and a non-stomatal term, ln($V_{cmax,app,leaf}/V_{cmax,app,T1}$). We flagged logs with ΔCO_2 below 2 µmol mol^{-1} or A ≤ 0 as signal-limited (12 of 24; 23 of 24 recorded before the stability criterion was met) and retained them with the flag [9].

Proline.

Leaf tissue (0.5 g FW in 10 mL) was quantified by acid ninhydrin with toluene partitioning; standards passed through the toluene step [14]. Because samples spanned 0–10 µg mL^{-1} we used a 0–40 µg mL^{-1} calibration (A_{520} = 0.005767·C + 0.08833; R^2 = 0.983; LOD 132 and LOQ 400 µg g^{-1} FW from 3.3σ/S and 10σ/S). A hierarchical Bayesian model in PyMC 5.28 [15] fitted standards and sample wells jointly. Extract concentrations were modelled as c_e ~ N(µ_level, σ_ext) while well-level measurements were modelled using A_well ~ Student-t(v = 4, b_0 + b_1c_e, σ_tech); where weakly informative priors were assigned to the model parameters. We compared cell-means, linear and hinge (µ = a + b·max(0, s − θ), θ ~ U(1, 5)) models by PSIS-LOO [16] and tested robustness under σ_ext ~ HalfNormal(10) and Gaussian wells. Sampling ran four chains of 3,000 draws (target acceptance 0.97): zero divergences, $\hat{R} \leq 1.001$, bulk ESS ≥ 2,500. Frequentist analyses complemented the Bayesian model using an exact Jonckheere–Terpstra trend test across all 113,400 label arrangements [17]. All analyses used either R 4.3.3 and Python 3.11 and the corresponding code are included as supplementary material.

Results

Residual proline shows a threshold response (H1; supported for these plants). Posterior median proline concentrations were recorded at 125, 141, 140, 122 and 50 µg g^{-1} FW for T1–T5, respectively (Fig. 1b). The T5 leaf had lower proline concentration than the control with a posterior median difference of − 75 µg g^{-1} FW, 95% CrI − 132 to − 12 and a posterior probability of a decrease of 0.985). In contrast the T2–T4 centered on zero with $P(\Delta < 0)$ ranging from 0.29 to0.55 (Fig. 1d). The hinge model estimated a change-point at $\theta = 3.9$ (95% CrI 2.4–4.7 with $P(\theta \geq 3) = 0.92$, and an estimated post-threshold slope of − 74 µg g^{-1} FW per treatment level (95% CrI − 199 to − 21). The hinge model provided better predictive performance than both the linear (ΔELPD = 2.2 ± 1.2) and cell-means (1.8 ± 0.8) models (Fig. 1c). The probability that T5 remained lower than T1 remained high (0.946 and 0.989) across alternative prior and likelihood specifications (Additional file 1: Table S1). The exact Jonckheere–Terpstra test provided limited evidence for an ordered trend (p = 0.061). However, the post-hoc contrast indicated that T5 was 85 ± 27 µg g^{-1} FW lower than the mean of T1-T4 ($t(5) = -3.16$, p = 0.025).

A first-principles C_i recomputation removes a widespread error.

Linear rescaling of C_i by 9/S, the correction applied in the sample workbook, can substantially bias C_i estimates when applied incorrectly. In the workbook, this correction placed 21 of 24 $C_i$values above ambient CO_2, which is thermodynamically impossible under net CO_2 uptake (Additional file 1: Fig. S1). In contrast, the first-principles pipeline described in the Methods returns physiologically bounded C_i values of 245–418 µmol mol^{-1} and formed the basis of Figs. 2 and 3.

Photosynthesis is limited by non-stomatal capacity, not diffusion (H2; not supported).

Net CO_2 assimilation (A) increased linearly with g_w in every leaf with no evidence of saturation (Fig. 3a). However, the response for T3 was much weaker with a slope of 48 (95% CI 13–82 µmol mol^{-1}) which is approximately half that observed for of T1, T2 and T4 (94–104 µmol mol^{-1}), with a marginal g_w × leaf interaction ($F(3,16) = 3.01$, p = 0.061). Median $L_$ ranged from 0.15 to 0.32 (Fig. 2d). The additive partition on matched rounds showed that most of the difference in A were attributed to non-stomatal effects, accounting for 78% of the T2 excess, 94% of the T3 deficit and 85% of the T4 excess (Fig. 3b). T3 assimilated 59% less CO_2 than T1 (mean ln-ratio − 0.89) with most of this difference arising from the non-stomatal component (− 0.83) while the diffusive component contributed only − 0.06. Across the 12 signal-adequate logs, $V_{cmax,app}$ correlated with g_v (Spearman $\rho = 0.90$, $p < 10^{-4}$), indicating that stomatal conductance and biochemical capacity moved together rather than one limiting the other. On day 2 of recovery, the median $V_{cmax,app}$in signal-adequate logs remained low (9.7–17.2 µmol m^{-2} s^{-1}), compared to the reported *in vivo* values for field-grown soybean [18], suggesting that stomatal and biochemical function had not fully recovered.

Timing of the diurnal maximum shifts later with severity in ordering, but not in confidence (H3; unresolved).

The quadratic peak in g_v occurred at 11.6 h for T1 (95% CI 7.6–15.9), 11.8 h for T2 (8.5–14.3) and 12.9 h for T4 (11.5–15.5) (Fig. 2b). T3 had no interior maximum and declined from the first round. Ordering matches the hypothesis; intervals overlap.

Proline does not predict carbon gain in these four leaves (H4; not supported). Diurnal integrated carbon gain was 60, 67, 18 and 104 mmol CO_2 m^{-2} for T1–T4, respectively. With proline uncertainty propagated, the treatment-level correlation was r = − 0.41 (95% CrI − 0.97 to 0.86, n = 4; Fig. 3c).

Discussion

Two mechanisms fit the T5 proline result and make different predictions for a replicated study. Faster ProDH-driven clearance in the most severely stressed plant predicts elevated ProDH transcript and proline oxidation with intact tissue [2]; loss of metabolically active tissue predicts low F_v/F and high electrolyte leakage in the same leaf [19]. The T5 extracts sit below the assay LOD, so the direction of the drop is credible but its magnitude is not.

The photosynthetic result argues against a purely stomatal account of early recovery. The linear A–g_v relationship, in isolation, would fit diffusion limitation; the tight covariance of $V_{cmax,app}$ with g_{sv} and the dominance of the non-stomatal term in leaf-to-leaf differences instead fit coordinated recovery, in which mesophyll conductance and biochemical capacity return in step with stomatal aperture [1, 6, 7]. The T3 leaf shows the non-stomatal failure most clearly. Two cautions limit this reading: at the lowest fluxes, cuticular conductance and IRGA noise bias C_i upward and V_{cmax} downward [9, 20]; and the one-point method cannot separate mesophyll from Rubisco constraints. Definitive attribution needs A/C_i curves and, ideally, chlorophyll fluorescence [21]. The T4 leaf's higher carbon gain than the control is unexpected under any linear stress model and merits explicit testing for hormetic overshoot in the replicated design.

Limitations

- **One plant per severity level.** Extracts and wells are sub-samples of one leaf per plant; posterior intervals describe within-leaf uncertainty and understate between-plant variance [22]. All contrasts describe these five plants.
- **Gas-exchange quality control.** T5 was not measured; 23 of 24 logs were recorded before the instrument's stability criterion was met; and 12 of 24 had ΔCO_2 below 2 µmol mol^{-1}.
- **Single recovery day.** Sampling on day 2 alone cannot separate rate from asymptote of recovery, cannot test hysteresis, and cannot resolve whether the T4 assimilation excess reflects overshoot or noise. Days 0, 2, 5, and 10 after re-watering are the natural targets.

Conclusions

This pilot supports a threshold, rather than a linear, model of residual leaf proline decline after re-watering in soybean, and suggests that early photosynthetic recovery is limited by coordinated stomatal and non-stomatal capacity rather than by stomata alone. This study contributes a methodological correction of a leaf-area rescaling error that inflated C_i above ambient in a widely used LI-6800 workbook. The findings apply to five plants and motivate a replicated study with ≥ 6 plants per level, continuous soil-water metrics, A/C_i curves, and repeated recovery-day sampling.

Declarations

Ethics approval and consent to participate

Not applicable. The study used greenhouse-grown *Glycine max* plants and did not involve human participants, human data or animal experiments.

Availability of data and materials

The raw LI-6800 file, the plate-reader export, the corrected gas-exchange dataset, the R and PyMC analysis code, and the model diagnostics will be deposited on Zenodo with a DOI on acceptance. The unmodified vendor Excel workbooks are archived unchanged; all derived data are generated by the accompanying scripts.

Competing interests

The authors declare that they have no competing interests.

Funding

This work was supported by internal funds of the Plant Holobiont Laboratory, Department of Botany and Zoology, Stellenbosch University and the National Research Foundation of South Africa Africa-Japan AJCR230626121654. SdS was funded by NRF Fellowship (PMDS250620324971)

Authors' contributions

IM conceived and supervised the study, secured funding, performed the reanalysis (Bayesian and frequentist models, first-principles gas-exchange recomputation), produced the figures, wrote the manuscript and finalised the code. **AK** contributed the initial datasets and funding source, and reviewed draft manuscript. **SdS** designed and executed the greenhouse treatments, performed the proline assay and the LI-6800 measurements, and contributed the initial datasets. All authors read and approved the final manuscript.

Acknowledgements

We thank the Plant Holobiont Laboratory team for constructive discussion and Ms Janette de Hutton (Lab Manager) for greenhouse support and Dr. Kerry Grey for training on the LI-6800. Analyses used

open-source software (R Core Team, PyMC developers, ggplot2, and patchwork).

Consent for publication

Not applicable.

References

1. Chaves MM, Flexas J, Pinheiro C. Photosynthesis under drought and salt stress: regulation mechanisms from whole plant to cell. Ann Botany. 2008;103:551–60. https://doi.org/10.1093/aob/mcn125.
2. Kiyosue T, Yoshiba Y, Yamaguchi-Shinozaki K, Shinozaki K. A nuclear gene encoding mitochondrial proline dehydrogenase, an enzyme involved in proline metabolism, is upregulated by proline but downregulated by dehydration in Arabidopsis. Plant Cell. 1996;8:1323–35. https://doi.org/10.1105/tpc.8.8.1323.
3. Szabados L, Savouré A. Proline: a multifunctional amino acid. Trends Plant Sci. 2009;15:89–97. https://doi.org/10.1016/j.tplants.2009.11.009.
4. Brodribb TJ, McAdam SAM. Abscisic Acid Mediates a Divergence in the Drought Response of Two Conifers. Plant Physiol. 2013;162:1370–7. https://doi.org/10.1104/pp.113.217877.
5. Tombesi S, Nardini A, Frioni T, Soccolini M, Zadra C, Farinelli D, et al. Stomatal closure is induced by hydraulic signals and maintained by ABA in drought-stressed grapevine. Sci Rep. 2015;5:12449. https://doi.org/10.1038/srep12449.
6. Flexas J, Bota J, Loreto F, Cornic G, Sharkey TD. Diffusive and Metabolic Limitations to Photosynthesis under Drought and Salinity in C 3 Plants. Plant Biol. 2004;6:269–79. https://doi.org/10.1055/s-2004-820867.
7. Galmés J, Medrano H, Flexas J. Photosynthetic limitations in response to water stress and recovery in Mediterranean plants with different growth forms. New Phytol. 2007;175:81–93. https://doi.org/10.1111/j.1469-8137.2007.02087.x.
8. Takahashi F, Suzuki T, Osakabe Y, Betsuyaku S, Kondo Y, Dohmae N, et al. A small peptide modulates stomatal control via abscisic acid in long-distance signalling. Nature. 2018;556:235–8. https://doi.org/10.1038/s41586-018-0009-2.
9. Márquez DA, Stuart-Williams H, Farquhar GD. An improved theory for calculating leaf gas exchange more precisely accounting for small fluxes. Nat Plants. 2021;7:317–26. https://doi.org/10.1038/s41477-021-00861-w.
10. Kauwe MGD, Lin Y, Wright IJ, Medlyn BE, Crous KY, Ellsworth DS, et al. A test of the 'one-point method' for estimating maximum carboxylation capacity from field-measured, light-saturated photosynthesis. New Phytol. 2015;210:1130–44. https://doi.org/10.1111/nph.13815.
11. Bernacchi CJ, Singsaas E, Pimentel C, Portis AR, Long SP. Improved temperature response functions for models of Rubisco-limited photosynthesis. Plant Cell Environ. 2001;24:253–9.

https://doi.org/10.1046/j.1365-3040.2001.00668.x.

12. Farquhar GD, von Caemmerer S, Berry JA. A biochemical model of photosynthetic CO2 assimilation in leaves of C3 species. Planta. 1980;149:78–90. https://doi.org/10.1007/bf00386231.
13. Farquhar GD, Sharkey TD. Stomatal Conductance and Photosynthesis. Annu Rev Plant Physiol. 1982;33:317–45. https://doi.org/10.1146/annurev.pp.33.060182.001533.
14. Bates LS, Waldren RP, Teare ID. Rapid determination of free proline for water-stress studies. Plant Soil. 1973;39:205–7. https://doi.org/10.1007/bf00018060.
15. Abril O, Andreani V, Carroll C, Dong L, Fonnesbeck C, Kochurov M, et al. PyMC: a modern, and comprehensive probabilistic programming framework in Python. PeerJ Comput Sci. 2023;9. https://doi.org/10.7717/peerj-cs.1516.
16. Vehtari A, Gelman A, Gabry J. Practical Bayesian model evaluation using leave-one-out cross-validation and WAIC. Stat Comput. 2016;27:1413–32. https://doi.org/10.1007/s11222-016-9696-4.
17. Jonckheere AR. A distribution-free K -sample test against ordered alternatives. Biometrika. 1954;41:133–45. https://doi.org/10.1093/biomet/41.1-2.133.
18. Bernacchi CJ, Morgan PB, Ort DR, Long SP. The growth of soybean under free air [CO2] enrichment (FACE) stimulates photosynthesis while decreasing in vivo Rubisco capacity. Planta. 2004;220:434–46. https://doi.org/10.1007/s00425-004-1320-8.
19. Hatsugai N, Katagiri F. Quantification of Plant Cell Death by Electrolyte Leakage Assay. BIO-PROTOCOL. 2018;8. https://doi.org/10.21769/bioprotoc.2758.
20. Boyer JS, Wong S, Farquhar GD. CO2 and Water Vapor Exchange across Leaf Cuticle (Epidermis) at Various Water Potentials. Plant Physiol. 1997;114:185–91. https://doi.org/10.1104/pp.114.1.185.
21. Sharkey TD, Bernacchi CJ, Farquhar GD, Singsaas E. Fitting photosynthetic carbon dioxide response curves for C3 leaves. Plant Cell Environ. 2007;30:1035–40. https://doi.org/10.1111/j.1365-3040.2007.01710.x.
22. Lazic SE. The problem of pseudoreplication in neuroscientific studies: is it affecting your analysis? BMC Neurosci. 2010;11:5. https://doi.org/10.1186/1471-2202-11-5.
23. Flexas J. Drought-inhibition of Photosynthesis in C3 Plants: Stomatal and Non-stomatal Limitations Revisited. Ann Botany. 2002;89:183–9. https://doi.org/10.1093/aob/mcf027.

Figures

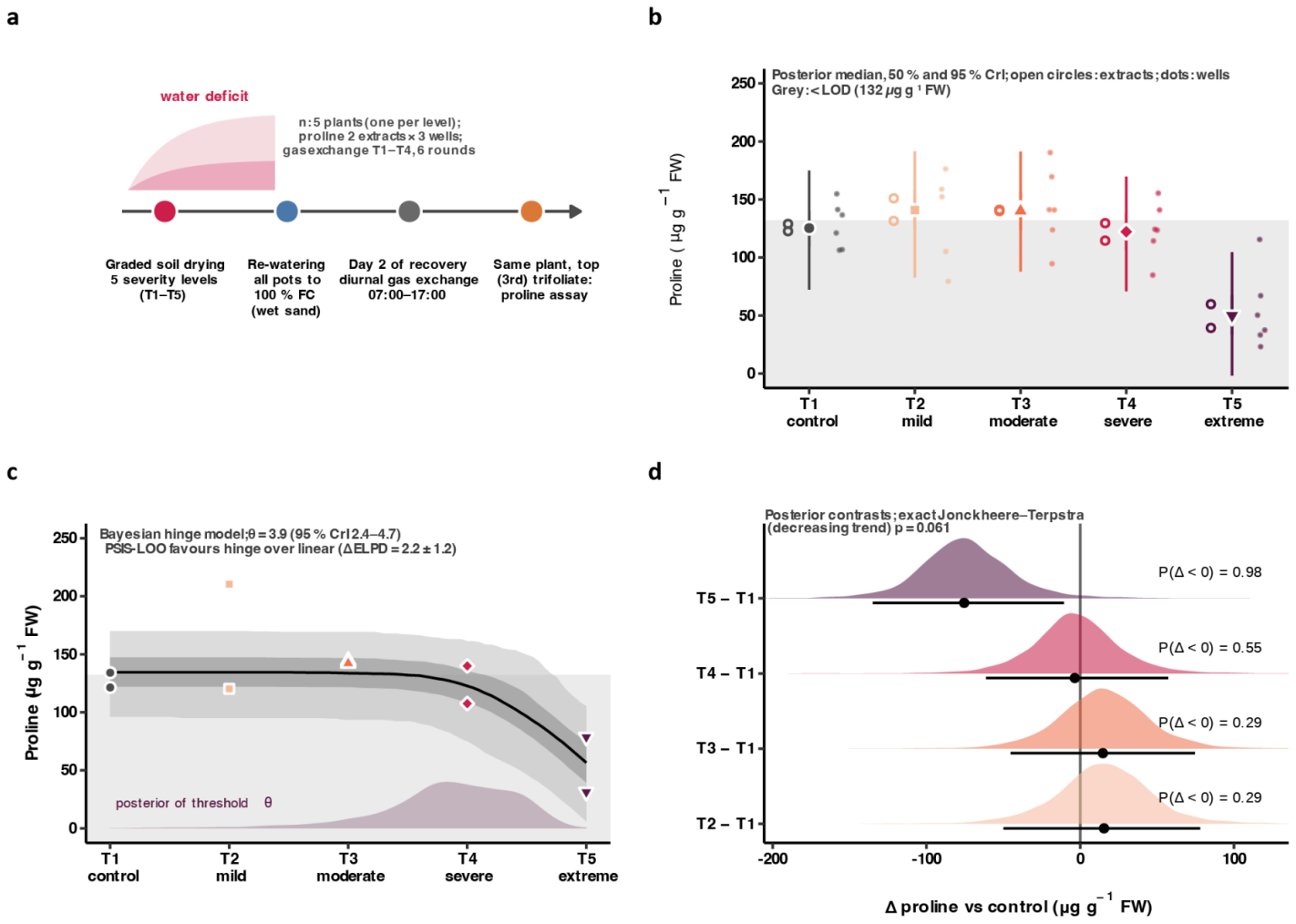

Figure 1

Residual leaf proline falls beyond a drought-severity threshold two days after re-watering. **a**Design: same-age soybean plants received one of five soil-drying levels (T1 control to T5 extreme), were re-watered to 100% field capacity (wet sand) and sampled on day 2; diurnal gas exchange and the proline assay came from the top (third) trifoliate of the same plant. **b** Proline (µg g^{-1} FW) from a joint hierarchical Bayesian model that fits calibration standards and sample wells together. Large symbols give posterior medians; thick and thin bars give 50% and 95% credible intervals (CrI). Open circles show extract-level posterior medians; small dots show individual wells. Grey shading marks values below the limit of detection (LOD, 132 µg g^{-1} FW); all samples lie below the limit of quantification (400 µg g^{-1} FW). **c** Hinge dose–response model, $\mu = a + b \cdot \max(0, \text{severity} - \theta)$. Black line and grey bands: posterior median, 50 % and 95% CrI; symbols: extract means; shaded density at base: posterior of the threshold θ. PSIS-LOO favoured hinge over linear (ΔELPD = 2.2 ± 1.2). **d**Posterior distributions of each level minus control, with medians, 95 % CrI and P(Δ < 0). With one plant per level, intervals describe within-leaf uncertainty for these plants, not variation among plants.

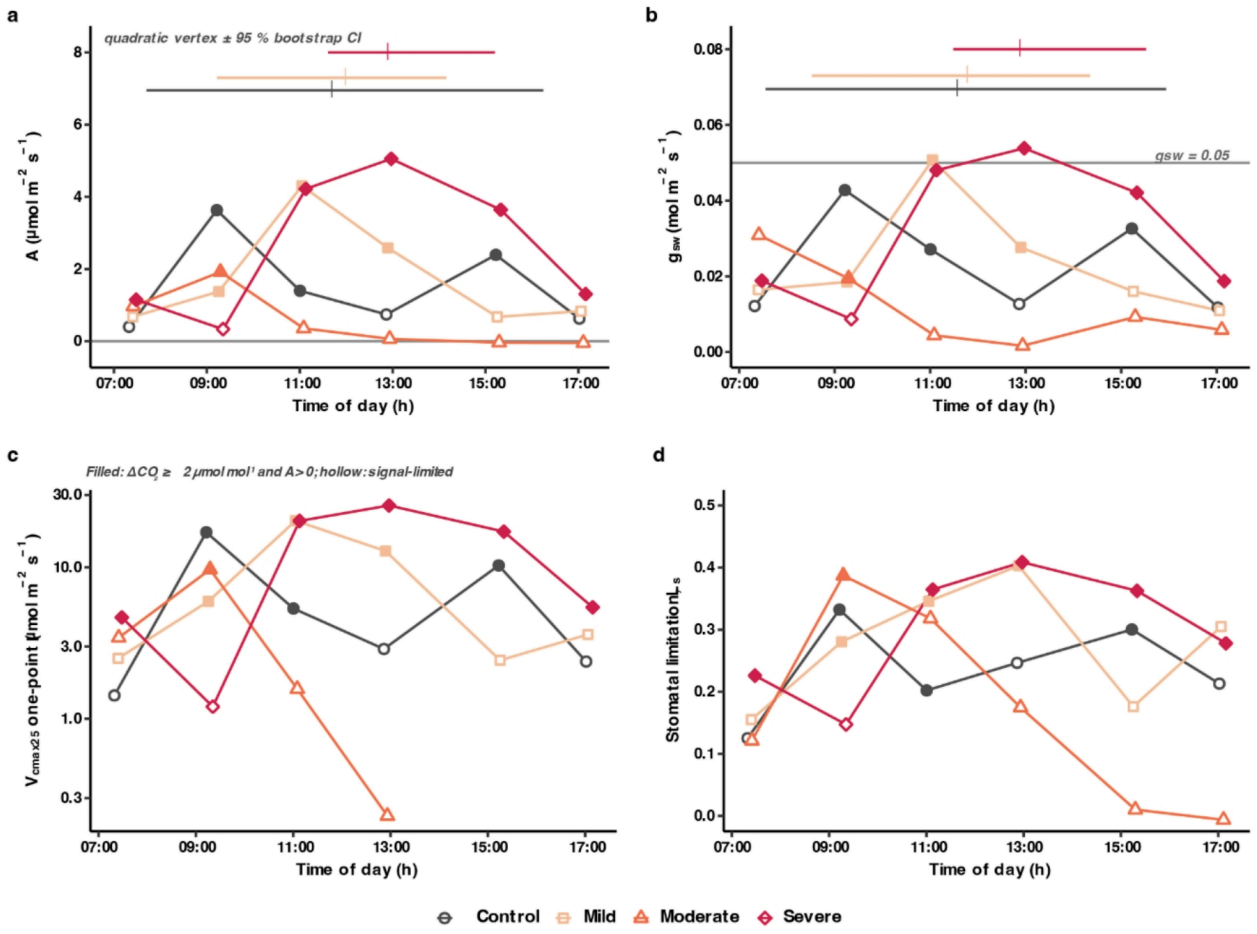

Figure 2

Diurnal photosynthetic recovery and its limitation on day 2 after re-watering. **a** Net CO_2 assimilation (A) of the T1–T4 leaves at PAR 1000 µmol m^{-2} s^{-1} and reference CO_2 415 µmol mol^{-1}, after first-principles leaf-area correction. Horizontal bars at the top show the vertex of a quadratic fit in time with its 95 % residual-bootstrap interval; T3 had no interior maximum. **b** Stomatal conductance to water vapour (g□□), recomputed from the LI-6800 equations; the line marks g□□ = 0.05 mol m^{-2} s^{-1}. **c**Apparent maximum carboxylation rate at 25 °C (V□□□□,app, log scale) from the one-point method. **d** Stomatal limitation L□ = 1 − A/A(C□ = C□). Filled symbols mark logs with $\Delta CO_2 \geq 2$ µmol mol^{-1} and A > 0; hollow symbols mark signal-limited logs. T5 was not measured. n = 1 leaf per level, 6 time points.

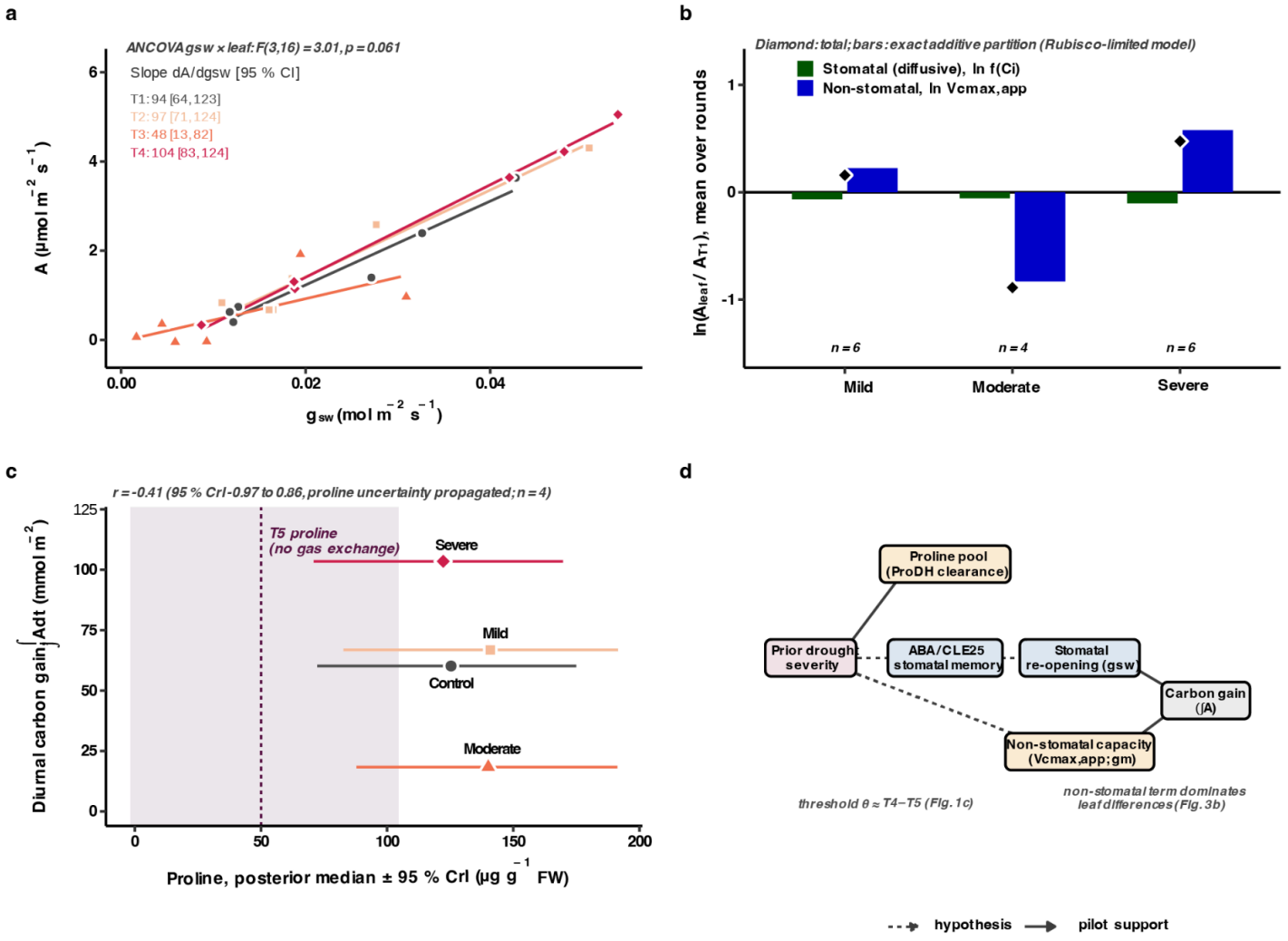

Figure 3

Non-stomatal capacity dominates leaf-to-leaf differences in early recovery. **a** A against g□□ for all 24 logs, with leaf-specific ANCOVA fits and slopes (dA/dg□□, µmol CO_2 mol^{-1} H_2O, 95 % CI); g□□ × leaf interaction F(3,16) = 3.01, p = 0.061. **b** Exact additive partition of ln(A_leaf/A_T1) into a stomatal (diffusive) term, ln f(C□), and a non-stomatal term, ln V□□□□,app, averaged over rounds in which both leaves had A > 0. Diamonds give the total log-ratio; positive values mean higher than T1. **c** Integrated diurnal carbon gain (∫A, 07:19–17:09) against posterior proline (median and 95 % CrI). Shaded band: T5 proline posterior (no gas-exchange record). r = −0.41 (95 % CrI −0.97 to 0.86, proline uncertainty propagated; n = 4). **d** Working model. Solid arrows: pilot support; dashed arrows: hypotheses for the replicated study. CLE25 acts upstream of foliar ABA [8].

Supplementary Files

This is a list of supplementary files associated with this preprint. Click to download.

- BMC02PythonPyMCprolinemodelsensitivityRhypothesisdrivenanalysisfigurescode.zip
- BMC02Posteriordraws4000modeldiagnosticsBayesiansummaryanalysislogExcelsummarytable.zip
- BMC01Additionalfile.docx